

UNCLASSIFIED

AD NUMBER
ADB041485
NEW LIMITATION CHANGE
TO Approved for public release, distribution unlimited
FROM Distribution authorized to U.S. Gov't. agencies only; Test and Evaluation; AUG 1979. Other requests shall be referred to Ballistic Research Lab., Attn: DRDAR-TSB, Aberdeen Proving Ground, MD 21005.
AUTHORITY
BRL ltr, 13 Nov 1986

THIS PAGE IS UNCLASSIFIED

AD BO 41485

AUTHORITY:

BRL etc.

13 NOV 86



THIS REPORT HAS BEEN DELIMITED
AND CLEARED FOR PUBLIC RELEASE
UNDER DOD DIRECTIVE 5200.20 AND
NO RESTRICTIONS ARE IMPOSED UPON
ITS USE AND DISCLOSURE.

DISTRIBUTION STATEMENT A

APPROVED FOR PUBLIC RELEASE;
DISTRIBUTION UNLIMITED.

② LEVEL III

AD-~~E-150303~~

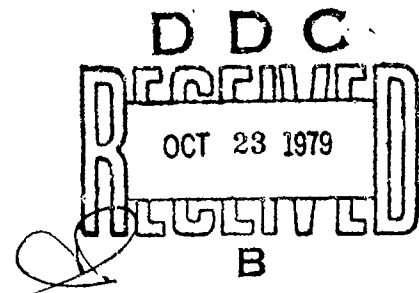
MEMORANDUM REPORT ARBRL-MR-02941

AD B041485

INFLUENCE OF MATERIAL VISCOSITY ON THE
THEORY OF SHAPED-CHARGE JET FORMATION

William P. Walters

August 1979



US ARMY ARMAMENT RESEARCH AND DEVELOPMENT COMMAND
BALLISTIC RESEARCH LABORATORY
ABERDEEN PROVING GROUND, MARYLAND

DDC FILE COPY

Distribution limited to US Government agencies only; Test and
Evaluation; All G 79. Other requests for this document must be
referred to Director, USA Ballistic Research Laboratory,
ATTN: DRDAR-TSB, Aberdeen Proving Ground, Maryland 21005.

79 09 26 011

1

Destroy this report when it is no longer needed.
Do not return it to the originator.

Secondary distribution of this report by originating
or sponsoring activity is prohibited.

Additional copies of this report may be obtained
from the Defense Documentation Center, Cameron
Station, Alexandria, Virginia 22314.

The findings in this report are not to be construed as
an official Department of the Army position, unless
so designated by other authorized documents.

*The use of trade names or manufacturers' names in this report
does not constitute indorsement of any commercial product.*

UNCLASSIFIED

SECURITY CLASSIFICATION OF THIS PAGE (When Data Entered)

REPORT DOCUMENTATION PAGE		READ INSTRUCTIONS BEFORE COMPLETING FORM
1. REPORT NUMBER Memorandum Report ARBRL-MR-02941	2. GOVT ACCESSION NO.	3. RECIPIENT'S CATALOG NUMBER
4. TITLE (and Subtitle) INFLUENCE OF MATERIAL VISCOSITY ON THE THEORY OF SHAPED-CHARGE JET FORMATION.	5. TYPE OF REPORT & PERIOD COVERED Final rept.	
7. AUTHOR(s) William P. Walters	6. PERFORMING ORG. REPORT NUMBER	
9. PERFORMING ORGANIZATION NAME AND ADDRESS U.S. Army Ballistic Research Laboratory (ATTN: DRDAR-BLT) Aberdeen Proving Ground, MD 21005	8. CONTRACT OR GRANT NUMBER(s)	
11. CONTROLLING OFFICE NAME AND ADDRESS U.S. Army Armament Research and Development Command U.S. Army Ballistic Research Laboratory (ATTN: DRDAR-BL) Aberdeen Proving Ground, MD 21005	10. PROGRAM ELEMENT, PROJECT, TASK AREA & WORK UNIT NUMBERS RDT&E 1L161102AH43	
14. MONITORING AGENCY NAME & ADDRESS (if different from Controlling Office) SBIE / AD-E430 303	12. REPORT DATE AUGUST 1979	
	13. NUMBER OF PAGES 43	
	15. SECURITY CLASS. (of this report) UNCLASSIFIED	
	15a. DECLASSIFICATION/DOWNGRADING SCHEDULE	
16. DISTRIBUTION STATEMENT (of this Report) Distribution limited to US Government agencies only; Test and Evaluation; Aug 1979. Other requests for this document must be referred to Director, US Army Ballistic Research Laboratory, ATTN: DRDAR-TSB, Aberdeen Proving Ground, MD 21005.		
17. DISTRIBUTION STATEMENT (of the abstract entered in Block 20, if different from Report)		
18. SUPPLEMENTARY NOTES		
19. KEY WORDS (Continue on reverse side if necessary and identify by block number) Viscosity Shaped-Charge Jet Collapse Visco-plastic Shaped-Charge Jet Modeling Viscous Effects		
20. ABSTRACT (Continue on reverse side if necessary and identify by block number) (MBA) The USSR has been engaged in viscosity measurements and visco-plastic material modeling for shock loaded materials since 1940. Shaped-charge jet or plate collapse models have been developed which are incompressible, one-dimensional, and viscid. In contrast, the USA employs a different modeling strategy where incompressible, inviscid flow is assumed for the simple one-dimensional jet or plate collapse models, and compressible, inviscid flow is assumed in the advanced axially symmetric hydrocode models. The USA advanced hydrocode models consider elastic-perfectly plastic stress-strain relationships or work hardening models.		

UNCLASSIFIED

(continued)

UNCLASSIFIED

SECURITY CLASSIFICATION OF THIS PAGE(When Data Entered)

(Item 20 Continued)

Whereas the USSR models jet or plate collapse, under shock loading conditions, via visco-plastic or rate-dependent models.

The USA establishes a jet-no-jet criterion and a jet cohesiveness criterion based on Mach number considerations or impinging angle considerations. Usually, the Mach number is based on an ambient bulk speed of sound value. The USSR, with their incompressible, viscid flow model, uses a critical Reynolds number criterion to define the jet-no-jet condition. *To use*

To utilize the USSR visco-plastic model, the constant (but unknown) viscosity coefficient must be determined. This parameter has been obtained from experimental data for various materials under shock loading conditions. The purpose of this report is to present the one-dimensional, USSR, viscous model for jet or plate collapse and the USSR criterion, for jet formation and jet cohesiveness. Also, viscosity values for various materials under shock loading conditions are given from the USSR open literature and from recent USA publications. *☆*

UNCLASSIFIED

TABLE OF CONTENTS

	Page
LIST OF ILLUSTRATIONS	5
LIST OF TABLES	7
I. INTRODUCTION	9
II. VISCOUS JET FORMATION MODEL	9
III. VISCOSITY DATA	16
IV. SUMMARY AND CONCLUSIONS	33
V. RECOMMENDATIONS	34
REFERENCES	35
DISTRIBUTION LIST	41

ACCESSION for		
NTIS	White Section	<input type="checkbox"/>
DDC	Buff Section	<input checked="" type="checkbox"/>
UNANNOUNCED		<input type="checkbox"/>
JUSTIFICATION _____		
BY _____		
DISTRIBUTION/AVAILABILITY CODES		
Dist.	AVAIL. and/or	SPECIAL
B		

LIST OF ILLUSTRATIONS

Figure	Page
1. Diagram of experimental arrangement (Reference 23)	17
2. Diagram of the experiments setup (Reference 18)	24
3. Measurements of the dynamic viscosity coefficient for different strain rates, Godunov (Reference 4)	30
4. Dynamic viscosity versus pressure, Barnes (Reference 28)	32

LIST OF TABLES

Table	Page
I. VISCOSITY DATA, MINEEV (Reference 21)	20
II. VISCOSITY OF WATER AND MERCURY , MINEEV (Reference 20)	22
IIIA. CALCULATED AND EXPERIMENTAL VISCOSITIES OF SEVERAL MOLTEN METALS NEAR THE MELTING POINT (Reference 22)	27
IIIB. VISCOSITY OF MOLTEN SODIUM AS AFUNCTION OF TEMPERATURE (Reference 22)	27
IV. VISCOSITY AS A FUNCTION OF STRAIN RATE, GODUNOV (Reference 24)	28

I. INTRODUCTION

The USSR has been engaged in the study of visco-plastic modeling of shock loaded materials since 1940 with the pioneering work of Il'yushin^{1,2} and Popov³. The USSR developed models to describe the jet formation process during the collisions of metal plates⁴⁻⁹. These models are analogous to those employed by the BRL¹⁰⁻¹², but the USSR has extended certain models to include the impact of asymmetric plates⁵ and viscous-flow effects^{4,5}. The basic BRL models¹⁰⁻¹² employ a one-dimensional, incompressible, inviscid flow model for the jet or plate collapse process, whereas the USSR models^{4,5} treat a one-dimensional, incompressible, viscous flow model for the shock loading of metal plates. As a result, the criterion used for predicting a jet-no-jet or jet cohesiveness condition is based on a critical Mach number or impingement angle criterion^{13,14}. Often the critical Mach number is calculated from the ambient bulk speed of sound value¹⁴. The USSR models, however, use a critical Reynolds number criterion to establish the jet-no-jet condition^{4,5}. The USSR viscous jet collapse model is presented in Section II.

In the axisymmetric hydrocode models used at BRL, compressible, inviscid flow is assumed, but the constitutive relationships are based on elastic-perfectly plastic or on work hardening models. The USSR utilizes rate-dependent, visco-plastic, stress-strain relationships^{3-5,15-17}. These relationships require a knowledge of the dynamic viscosity coefficient, and many USSR investigators^{1-4,18-25} have deduced the viscosity from experimental measurements under shock loading conditions. Some Western World viscosity values have also been obtained²⁶⁻³⁰ from shock loading experiments.

The dynamic viscosity is dependent on many parameters, primarily strain rate, pressure, and temperature and can range from 10^{-3} Pa-s for metals in the liquid state²⁶ to 10^7 Pa-s for very low strain rates⁴. However, for a given pressure, temperature, and strain rate, all materials may have nearly the same viscosity¹⁸ and behave as Newtonian fluids (for a fixed strain rate)^{1-4,18-23}. A summary of the experimental and theoretical values of the viscosity coefficients are given in Section III. The references cited relate to viscosity data, visco-plastic modeling, shock-wave propagation and dislocation dynamics. The cited references represent a partial bibliography which is far from complete.

II. VISCOUS JET FORMATION MODEL

Godunov, Deribas, and Mali⁴ modified the jet formation equations of References 10-12 to include the viscosity of metals under symmetrical dynamic loads. The resulting equations are analogous to the inviscid models¹⁰⁻¹² and include extra terms resulting from viscous flow considerations. All other assumptions are the same as employed by Reference 10.

**References are listed on page 35*

The equations from Reference 4 are repeated here since this author feels that some of the results given in Reference 4 are in error. Also, an outline of the derivation and the analogy to References 10-12 are presented.

Birkhoff¹⁰ gives

$$V = V_0 \left\{ \frac{\cos \frac{1}{2} (\beta - \alpha)}{\sin \beta} + \frac{\cos \frac{1}{2} (\beta - \alpha)}{\tan \beta} + \sin \frac{1}{2} (\beta - \alpha) \right\} \quad (1)$$

and

$$\frac{D}{\cos \alpha} = V_0 \frac{\cos \frac{1}{2} (\beta - \alpha)}{\sin (\beta - \alpha)}, \quad (2)$$

where the notation of Reference 4 will be converted to the notation used in Reference 10, and

V is the forward jet velocity,

V_0 is the velocity of the liner,

D is the speed of the plane detonation wave traveling parallel to the jet axis,

2α is the initial conical apex angle,

and 2β is the collision angle.

D' is defined to be the speed of the detonation wave traveling along the liner or

$$D' = \frac{D}{\cos \alpha}. \quad (3)$$

The combination of Equations 1, 2, and 3 yields

$$V = D' \sin (\beta - \alpha) \left[\frac{1 + \cos \beta}{\sin \beta} + \tan \frac{1}{2} (\beta - \alpha) \right]^{\dagger}. \quad (4)$$

[†]This result disagrees with Equation 1 of Godunov⁴ apparently due to an error by Godunov⁴.

The mass per unit length of the jet is given by

$$m_j = \frac{m(1 - \cos \beta)}{2}, \quad (5)$$

where m is the mass per unit length of the collapsing liner. The jet mass equation is identical to that given by Birkhoff¹⁰. Also, Godunov⁴ gives, for the jet velocity,

$$V_j = V_o \frac{(1 + \cos \alpha)}{\sin \alpha}, \quad (6)$$

when the detonation wave moves normal to the surface of the liner or $\beta = \alpha$. This equation was given by Birkhoff¹⁰.

For the case of a liner being collapsed by a detonation wave moving along its surface,

$$V_j = V_c + V' = D \frac{\sin (\beta - \alpha)}{\sin \beta} \left[1 + \frac{\cos (\frac{\beta + \alpha}{2})}{\cos (\frac{\beta - \alpha}{2})} \right], \quad (7)$$

where V_c is the velocity of the stagnation point, and V' is the liner flow velocity or

$$V_c = D \frac{\sin (\beta - \alpha)}{\sin \beta}, \quad (8)$$

and

$$V' = D \frac{\sin \beta - \sin \alpha}{\sin \beta}. \quad (9)$$

Equations 8 and 9 follow from De Fourneaux's¹² Equations 52 and 53, respectively, for the stationary or steady-state case where $\beta = \alpha + \phi$ and ϕ is the plate bending angle.

Godunov⁴ proposed a method to determine the influence of viscosity on the jet formation process. In particular, a jet formation criterion is derived which is based not on taking account of the compressibility, as in References 31 or 13, or on taking account a critical Mach number, as in Reference 14, but on taking into account the viscous properties of metals. An approximate method is used to estimate the effect of viscosity in the plane problem of jet collisions. The fluid is incompressible, the motion irrotational and steady-state, and the coefficient of viscosity is constant. Then the solutions of the Euler equations

automatically satisfy the Navier-Stokes equations of motion and the whole difference between the problems of ideal and viscous jet collisions is the conditions on the free surface of the jet. For the flow fields to agree in these problems, some forces must be applied to the free surface in the viscous flow case. The taking into account of the influence of these forces on the flow from collisions between jets of an ideal fluid will be the estimate, in a first approximation, of the influence of viscosity in the jet formation problem⁴.

The components of the viscous stress tensor in an incompressible fluid are defined by

$$\sigma_{ik} = \mu \left(\frac{\partial u_i}{\partial x_k} + \frac{\partial u_k}{\partial x_i} \right), \quad (10)$$

where u_i are the velocity components, x_i are the Cartesian coordinates, and μ is the viscosity coefficient. The modulus of the viscous force is taken to be

$$|\sigma_x + i \sigma_y| = 2\mu \frac{u_1}{R}, \quad (11)$$

where u_1 is the modulus of the complex velocity, $u_1 - iu_2$, and R is the radius of curvature of the free surface of the fluid. Then, Reference 4 postulates that, if the decelerating effect of the surface viscous forces on the reverse jet (or slug) will equal the computed value of the reverse jet force, then it is natural to expect that the reverse jet will not be formed. The horizontal component of the viscous force acting on the free surface of the reverse jet over the angular variation from β to $\pi/2$ is

$$M' = 2\mu u_1 (1 - \sin \beta), \quad (12)$$

and, since the same force per unit length acts on the opposite symmetric part of the free surface of the reverse jet, the total deceleration force per unit length is

$$M = 2 M' = 4\mu u_1 (1 - \sin \beta). \quad (13)$$

Now, consider the symmetric collision of two plane fluid jets. For an ideal, incompressible fluid the reverse jet force per unit length is given by Reference 32 as

$$M_1 = 2\rho \delta_1 u_1^2 \sin^2 \beta, \quad (14)$$

where ρ is the density, δ_1 is the thickness of the colliding jets, u_1 is the reverse jet velocity in a coordinate system coupled to the

stagnation point, and 2β is the collision angle. Godunov⁴ assumes that viscous fluid jets collide and form a reverse jet and the viscous fluid flow domain coincides with the analogous domain for an ideal fluid. As mentioned previously, the solutions of the Euler equations satisfy the Navier-Stokes equations of motion; the differences in these flows are attributed to the conditions on the free surface.

The formation of a reverse jet is possible only if the horizontal component of the viscous force, acting on the free surfaces of the reverse jet, is less than the force resulting from the symmetric collision of two plane fluid jets. From Equations 13 and 14, this inequality is established:

$$2\rho \delta_1 u_1^2 \sin^2 \beta > 4\mu u_1 (1 - \sin \beta). \quad (15)$$

By letting the Reynolds number be defined as

$$Re = \frac{\delta_1 u_1 \sin^2 \beta}{\nu (1 - \sin \beta)}, \quad (16)$$

where $\nu = \mu/\rho$ is the kinematic viscosity, the criterion for jet formation is

$$Re > 2. \quad (17)$$

Next, the jet velocity for a viscous flow is computed for the case where a reverse jet exists. A simple force balance yields

$$2\rho \delta_1 u_2^2 \sin^2 \beta = 2\rho \delta_1 u_1^2 \sin^2 \beta - 4\mu u_1 (1 - \sin \beta), \quad (18)$$

where u_2 now represents the reverse jet velocity in a coordinate system coupled to the stagnation point and u_1 is the liner flow velocity. From Equation 18 and Equation 9, the reverse jet velocity, u_2 , for the impact of two flat plates is given by

$$u_2 = D \left(\frac{\sin \beta - \sin \alpha}{\sin \beta} \right) \sqrt{1 - \frac{2\nu (1 - \sin \beta)}{\delta_1 D \sin \beta (\sin \beta - \sin \alpha)}}, \quad (19)$$

and the jet velocity in a fixed (laboratory) coordinate system is obtained by adding V_c from Equation 8 to Equation 19, or for D perpendicular to the liner,

$$u_j = V_c + u_2$$

$$= D \frac{\sin(\beta - \alpha)}{\sin \beta} \left[1 + \frac{\cos(\frac{\beta + \alpha}{2})}{\cos(\frac{\beta - \alpha}{2})} \sqrt{1 - \frac{2\nu(1 - \sin \beta)}{\delta_1 D \sin \beta (\sin \beta - \sin \alpha)}} \right]. \quad (20)$$

For plates in parallel, or when $\alpha = 0$, Equation 20 becomes

$$u_j = D \left[1 + \sqrt{1 - \frac{2\nu(1 - \sin \beta)}{\delta_1 D \sin^2 \beta}} \right]. \quad (21)$$

Equation 20 (or Equation 21, if $\alpha = 0$) gives the shaped-charge jet velocity for viscous flow effects.

When the detonation wave velocity is directed along the liner, i.e., $D' = D/\cos \alpha$ from Equation 3, Equation 20 becomes, for D' directed along the jet

$$u_j = \frac{D' \sin(\beta - \alpha)}{\cos \alpha \sin \beta} \left[1 + \frac{\cos(\frac{\beta + \alpha}{2})}{\cos(\frac{\beta - \alpha}{2})} \sqrt{1 - \frac{2\nu(1 - \sin \beta) \cos \alpha}{\delta_1 D' \sin \beta (\sin \beta - \sin \alpha)}} \right], \quad (22)$$

which is identical to Equation 21 when $\alpha = 0$.

For the detonation wave impacting normal to the liner surface, the jet velocity from Equation 22 for $\beta = \alpha$ and, by using Equation 2, becomes

$$u_j = \frac{V_o}{\sin \alpha} \left[1 + \cos \alpha \sqrt{1 - \frac{4\nu(1 - \sin \alpha)}{\delta_1 V_o \sin 2 \alpha}} \right]. \quad (23)$$

Now, Equations 23, 22, and 20 relax to the inviscid jet relationships given by Equations 6, 4, and 7, respectively, for the detonation wave directed along the liner when $v = 0$.

The values of the metal viscosity coefficients in shaped-charge jet flows must be used in conjunction with the strain rates achievable which can be estimated as

$$\dot{\epsilon} \approx \frac{\Delta u}{\Delta s} \approx \frac{u_1 (\pi - \beta)}{R (\pi - \beta)} = \frac{u_1 \pi}{2 \delta_1 \sin^2 \beta}, \quad (24)$$

where a change in velocity results from the rotation of the velocity vector, u_1 , through the angle, $\pi - \beta$, over the path, $\Delta s = R (\pi - \beta)$. The radius of curvature, R , is given as

$$R = \frac{2 \delta_1}{\pi} \sin^2 \beta \quad (25)$$

from Reference 9 where the β given in Reference 9 corresponds to 2β in the notation of Reference 4.

Finally, experimental jet data can be used to estimate the steady-state viscosity coefficient, where, from Equation 18,

$$\mu = \left[1 - \left(\frac{u_2}{u_1} \right)^2 \right] \frac{\rho u_1 \delta_1 \sin^2 \beta}{2 (1 - \sin \beta)}. \quad (26)$$

Also, from Equation 15, the critical velocity of the liner in the direction of the stagnation point, at which a failure to jet will occur, is given by

$$u_1^{cr} = \frac{2 (1 - \sin \beta) v}{\delta_1 \sin^2 \beta}. \quad (27)$$

Finally Equations 17, 20, 26, and 27 define the USSR criterion for jet formation and give the shaped-charge jet velocity for viscous effects. Again, Godunov⁴ was the major source of this information. This model has been extended to asymmetric collisions in Reference 5. Reference 6 derives an expression for the stagnation point velocity, in steady state, as a function of the charge-to-mass ratio for inviscid flow.

III. VISCOSITY DATA

The earliest known USSR viscosity measurements were from Il'yushin^{1,2} and Popov³ as reported in Reference 18. The material behavior is modeled as a rate-dependent process and the visco-plastic relationship between the stress, σ , and the strain rate, $\dot{\epsilon}$, is given by

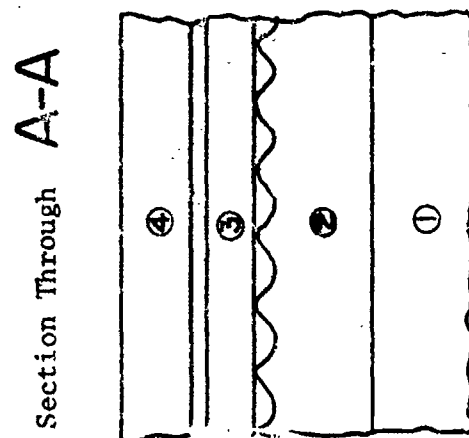
$$\sigma = \sigma_y + \mu \dot{\epsilon},$$

where σ_y is the yield stress and μ is the dynamic viscosity coefficient. Thus, knowledge of the viscosity coefficient, which is assumed to be constant, is required for the application of the visco-plastic, stress-strain rate relationship. As will be seen, the viscosity coefficient is, in reality, not constant but dependent primarily on the pressure, temperature, and strain rate. Nonetheless, Il'yushin^{1,2} and Popov³ performed experiments on cylindrical specimens tested in a pneumatic impact tester and concluded that the viscosity coefficients of various steels lie in the interval of 3×10^4 to 14×10^4 Pa-s and the viscosity coefficients of various aluminums lie in the interval of 3×10^4 to 4×10^4 Pa-s.

Another method of determining the viscosity of continuous media, based on the experimental investigation of the development of small perturbations in a shock front, was proposed in Reference 23.

Sakharov²³ attempted to investigate the stability of a plane shock wave in a substance in a condensed state and to deduce the mechanical properties of the substance under conditions of high pressure and temperature behind the shock front. The experimental arrangement is depicted in Figure 1 from Reference 23. The experiment was designed to satisfy the boundary and initial conditions associated with theoretical calculations performed for a linear approximation ($ka \ll 1$ where a is the perturbation amplitude, $k = 2\pi/\lambda$ and λ is the wavelength). For $t = t_0$, the surface of the shock front is assumed to have a sinusoidal profile and the flow behind and ahead of the shock front is constant.

From Figure 1, a plane shock wave, originating from the detonation of the explosive charge, passes through the sinusoidal grooves of the disc (2) into the wedge (3). Perturbations appear on the wedge of the same wavelength as the grooves in the disc. The wedge and the disc are made of the material under investigation. On further propagation of the shock wave through the wedge which is carrying the perturbation, the shock wave enters the gap between the tapered surface of the wedge and the plastic plate, where the perturbations are recorded by a fluorometric device SFR-2M. By using slits which are perpendicular to the direction of the wedge taper, a single perturbation can be recorded in one experiment at several successive times²³.



1. Explosive Charge
2. Grooved Disc
3. Wedge
4. Plastic Plate

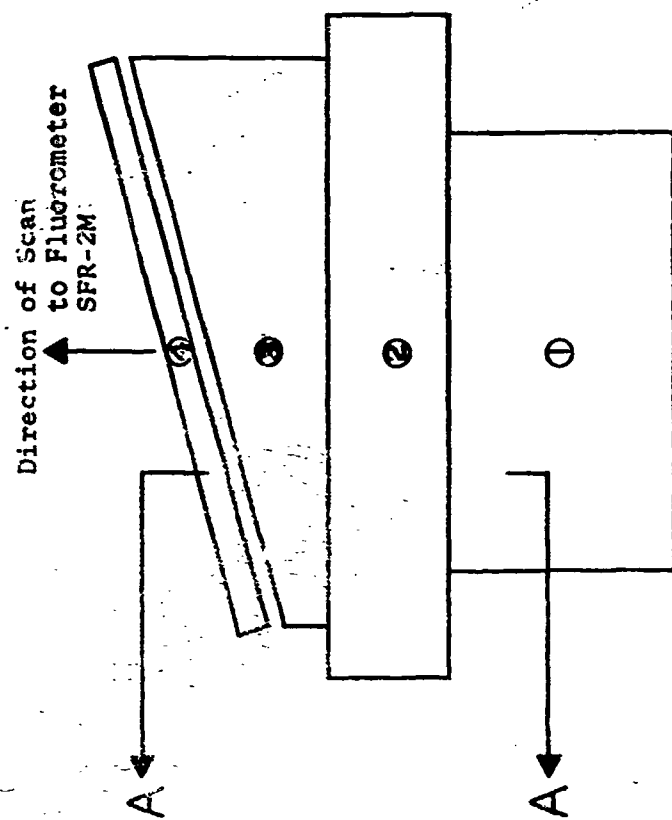


Figure 1. Diagram of experimental arrangement (Reference 23).

By choosing sufficiently large values for the length and diameter of the explosive charge, the diameter of the disc, etc., it is possible to approximately insure a uniform flow behind the shock front²³.

The method of producing the perturbations destroys the uniformity of flow behind the shock front at distances of order a_0 , the initial amplitude, which leads to errors of the second order with respect to ka_0 . In each case, the effect of deviations from the calculated conditions in the experimental arrangements was studied experimentally, and the experimental results were subjected to corrections²³.

Sakharov²³ studied the development of perturbations by shock waves in aluminum alloy AL-9 (90% aluminum). The pressure at the wave front was 3.14×10^{10} Pa, the temperature was 603°K, and the density was 3.4 Mg/m^3 . These parameters were obtained from an assumed equation of state³³. The experimental curves of the development of perturbations were obtained for wavelengths of 0.1, 0.2, and 0.33mm and initial perturbation amplitudes of $ka_0 = 0.29$ to 1.74. In the experiments using different wavelengths, all linear parameters of the experimental assembly were scaled with the wavelength to eliminate the effect of boundary conditions on the required dependence of λ . The viscosity coefficient for the AL-9 aluminum alloy was calculated to be $2 \times 10^3 \text{ Pa-s}$ behind the shock front²³. Increasing the shock wave pressure up to $1.01 \times 10^{11} \text{ Pa}$ changes the coefficient of viscosity weakly, but it does not exceed 10^4 Pa-s^{23} . The perturbation development curves for different values of the wavelength agreed for the case of aluminum powder with an initial density of 0.68 Mg/m^3 . It is possible that this indicates melting of the aluminum behind the shock front, since the use of a powdered material leads to considerable heating behind the shock front²³.

Later Mineev²¹ continued the experiments in order to obtain the viscosity of aluminum, lead, and sodium chloride at pressures of 10^{10} to $2 \times 10^{11} \text{ Pa}$. It was shown that, when complete geometric similarity is maintained in the experiments (with respect to the wavelength of the disturbances), the influence of viscosity reduces to a phase shift between the curves of disturbance amplitude versus time, thereby showing the development of disturbances having various wavelengths. However, under certain thermodynamic conditions, the development of a disturbance is independent of the wavelength. This is associated with the melting of the test material behind the shock front.

In the actual experiments, the development of disturbances of two wavelengths, namely, $\lambda_1 = .01 \text{ mm}$ and $\lambda_2 = .02 \text{ mm}$ with relative initial amplitudes of $ka_0 = 0.63$ and 1.89, respectively, was considered in two geometrically similar arrangements with respect to λ .

The dynamic viscosity, μ , was obtained from the formula[†]

$$\mu = \rho D \Delta x / k a_0 (1/\lambda_1 - 1/\lambda_2),$$

where ρ is the density of the material behind the unperturbed shock front, D is the wave speed of the unperturbed shock front, and $x = S(t)/\lambda$, where S is the path traveled by the shock wave. In fact, Δx is the phase shift of the curves showing the development of disturbances with λ_1 and λ_2 , plotted with coordinates $y = a(t)/a_0$ and x . Here, $a(t)$ and a_0 are the running and initial disturbance amplitudes, respectively²¹.

Table I, from Reference 21, lists the values of the dynamic viscosity for lead and aluminum under various pressures, compressions, and temperatures. The viscosity values are given with a maximum error band due to the inaccuracy in the determination of Δx . Again, equations of state were used to determine the thermodynamic properties³³⁻³⁵.

Also, disturbances in the shock front in sodium chloride were investigated for two cases corresponding to a pressure of 240×10^8 Pa, a compression of 1.44, and a temperature of 1550°K, and a pressure of 205×10^8 Pa, a compression of 1.31, and a temperature of 2620°K. Again, empirical equations of state were required³⁶. In the first case, the viscosity was deduced to be $2 \pm 1 \times 10^4$ Pa-s and less than 10^3 Pa-s in the second case.

From the data presented in Table I, Mineev²¹ states that the viscosity values of aluminum and lead behind the shock front at pressures of 310 and 350×10^8 Pa are nearly equal at $2-4 \times 10^3$ Pa-s. Under these conditions, the aluminum and lead are deformed by 174% at a deformation rate of 10^7 s⁻¹. The weak dependence of the viscosity on the nature of the substance was also reported in References 1-3, which showed that, under dynamic loading conditions characterized by deformation rates of 6×10^2 to 6×10^3 s⁻¹, aluminum and various grades of steels behave as viscous liquids with $\mu = 3-4 \times 10^4$ Pa-s.

The deformation rate given by Mineev²¹ was of the order $\dot{\epsilon} = \frac{4\pi^2 a_0 D}{\lambda^2}$,

and the viscosity of aluminum at 310×10^8 Pa remained constant, within the limits of the experimental scatter, for deformation rates between

[†]In Mineev's²¹ formula for the dynamic viscosity, the initial amplitude a_0 does not appear. The a_0 was inserted by the author to enable the viscosity to have the correct units. The term, $k = 2\pi/\lambda$, is constant according to Reference 21, but it is unclear as to which value of λ (λ_1 or λ_2) is to be used. However $x = S(t)/\lambda$ and the term, $\Delta x/k$, results in the cancellation of λ . However k must be nondimensional, and it is assumed that Mineev meant k to be $\frac{2\pi a_0}{\lambda}$.

TABLE I. VISCOSITY DATA, MINEEV (Reference 21)

Material	Ratio of normal density to initial density	Pressure (Pa x 10 ⁻⁸)	Compression	Temperature (°K)	Dynamic Viscosity (Pa-s x 10 ⁻³)
Al	1	310	1.26	630	2 ± 0.5
Pb	1	350	1.36	1400	3.7 ± 1.4
Al	1	680	1.42	1600	10 ± 4
Al	1	1050	1.56	3500	7 ± 2
Al	1	2020	1.83	10,100	< 2
Al	1.23	275	1.18	1700	1 ± 0.5
Al	1.43	245	1.13	2600	< 0.2
Al	4	120	0.87	4600	< 0.2
Pb	1	410	1.38	1700	15 ± 2
Pb	1	1240	1.65	7000	< 30
Pb	1	2500	2.06	20,000	< 13

4×10^5 to $8 \times 10^6 \text{ s}^{-1}$ ^{21,23}. This would suggest, from the available experimental data, that the viscosity of aluminum is independent of the rate of deformation and hence the viscosity is Newtonian. Mineev²¹ also showed that aluminum exists in the plastic state behind the disturbed shock front.

Thus, the viscosity of aluminum reported in Reference 21 is an order-of-magnitude smaller than the value reported in References 1 - 3 at $310 \times 10^8 \text{ Pa}$ due solely to the difference in temperature between the two experiments. When the shock wave pressure is increased from $310 \times 10^8 \text{ Pa}$ to $1050 \times 10^8 \text{ Pa}$, the viscosity of aluminum increases slightly but remains less than 10^4 Pa-s . More exact values of the viscosity were not obtained since the value of Δx could not be resolved smaller than 0.02 - 0.03. Also, there was evidence that large pressure gradients behind the disturbed shock front were present due to large initial disturbances.

Mineev²⁰ used the same experimental arrangement to obtain the dynamic viscosity of water and mercury under shock loading conditions at pressures between 40×10^8 and $440 \times 10^8 \text{ Pa}$. The viscosity was approximately the same ($\sim 10^3 \text{ Pa-s}$) as the value for shock compressed solids^{1-3,21,23}. For both water and mercury, the coefficient of viscosity increases with increasing pressure (or increasing density) and decreases with increasing temperature. Under shock loading conditions, the density and temperature increase simultaneously making it difficult to accurately determine the effect of only pressure or temperature on the dynamic viscosity. The viscosity values of water and mercury under the test conditions of Mineev²⁰ are listed in Table II. From the table, it follows that the deformation was of the order 20 to 140 percent and the rate of deformation was $1-6 \times 10^5 \text{ s}^{-1}$. Under these conditions, in a range of pressures from $80 - 105 \times 10^8 \text{ Pa}$ and temperatures of $700 - 1200^\circ\text{K}$, the coefficient of dynamic viscosity of water is practically constant ($\mu \sim 10^3 \text{ Pa-s}$). The viscosity values of water and mercury are about the same as the viscosity of shock-compressed aluminum and lead at pressures of $300 - 400 \times 10^8 \text{ Pa}$. It is significant that the viscosity values for aluminum and lead were obtained at approximately the same values of deformation and deformation rate as those of shock-compressed water and mercury^{20,21,23}. According to Reference 20, this explains the approximate equality of the coefficients of dynamic viscosity of shock-compressed aluminum, lead, sodium chloride, water, mercury, and other materials, cited in References 21 and 23, which are very different under normal conditions. The number of defects produced during the deformation of solids depends weakly on the type of material undergoing deformation and is basically determined by the deformation and deformation rate. Since the experiments of References 20, 21, and 23 had nearly equal values of the deformation and deformation rate, equal numbers of defects can be expected to appear and, as a result, approximately equal values of the dynamic viscosity coefficients can be expected.

TABLE II. VISCOSITY OF WATER AND MERCURY, MINEEV (Reference 20)

Material	Pressure ($\times 10^{-8}$ Pa)	Compression	Temperature ($^{\circ}$ K)	Wave velocity of the unperturbed shock front (km/s)	Deformation rate (%)	Deformation rate ($\times 10^{-5}$ s $^{-1}$)	Viscosity ($\times 10^{-3}$ Pa-s)
Water	40	1.44	470	3.61	110	2.5	< 0.08
Water	80	1.59	700	4.64	44	1.3	1.8 ± 0.2
Water	120	1.70	980	5.40	30	1.0	2.9 ± 0.4
Water	150	1.76	1200	5.88	15	2.7	2.2 ± 0.4
Mercury	440	1.39	-	3.39	140	6	0.8 ± 0.2

At a pressure of 40×10^8 Pa, the coefficient of dynamic viscosity of water is at least an order-of-magnitude smaller than the viscosity value at 80×10^8 Pa. Under certain thermodynamic conditions behind the shock-wave front, the development of perturbations does not depend on λ , and this indicates a sharp decrease in the viscosity of the material. In other words, the shock wave front breaks down due to the increasing viscosity of the water in the shock-wave front. Also, at 40×10^8 Pa of pressure, the water may exist in the liquid and ice phase, whereas the water is completely liquid above a pressure of 40×10^8 Pa²⁰.

It is also worthy of noting that the viscosity coefficient depends on the shock relaxation time, $\tau \sim \epsilon^{-1}$ or $\mu = \rho \tau (C_0^2 - C_\infty^2)$, where C_0 and C_∞ are the equilibrium and non-equilibrium speeds of sound. For $C_0^2 \gg C_\infty^2$, $\rho = 1 \text{ Mg/m}^3$, $C_0 \sim 10^6 \text{ mm/s}$, and $\tau \sim 10^{-5} \text{ s}$, $\mu \sim 10^4 \text{ Pa-s}$, which is in approximate agreement with the experimental results²⁰.

Mineev²⁰ also points out that the shock-wave thickness varies strongly with pressure, and the viscosity of water can vary from 10^{-3} to 0.3 Pa-s for pressures between 0 to $20 \times 10^8 \text{ Pa}$.

Harlow and Pracht²⁷ of LASL report a viscosity coefficient of about 10^4 Pa-s for shock loaded aluminum in the later stages of the experiment, after some cooling had taken place. The viscosity coefficient could drop two orders-of-magnitude corresponding to maximum heating of the metal. Also, in Reference 27 the dynamic viscosity of iron was deduced to be around $2 \times 10^3 \text{ Pa-s}$. This value is of the right order-of-magnitude to explain the decrease in jet velocity near the critical angle for a collapsing shaped-charge liner²⁷.

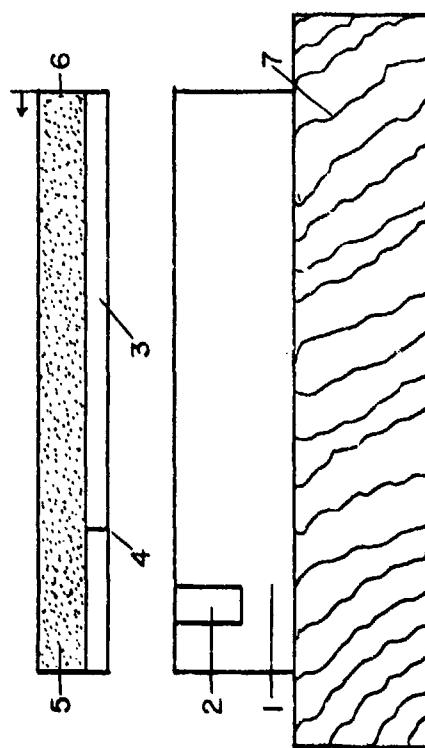
Burkhardt²⁶ deduced the dynamic viscosity of liquid metals near the melt temperature and found $\mu = 10^{-3} \pm 1 \text{ Pa-s}$ for aluminum, copper, and steel from an investigation of the boundary surfaces of explosively welded metals at various Reynolds numbers.

Specifically, for liquid metals near the melting temperature, μ was $2.9 \times 10^{-3} \text{ Pa-s}$ for aluminum, $3.3 \times 10^{-3} \text{ Pa-s}$ for copper, and $2.8 \times 10^{-3} \text{ Pa-s}$ for steel.

Godunov¹⁸ investigated the viscosity of metals under impact in the explosive-welding regime. By means of the method of fixed lines, it was shown that the viscosity is inversely proportional to the particle displacement in the direction of the contact-point velocity. The particle displacements were measured by optical metallography. Values of the viscosity coefficients were estimated for aluminum, copper, and steel.

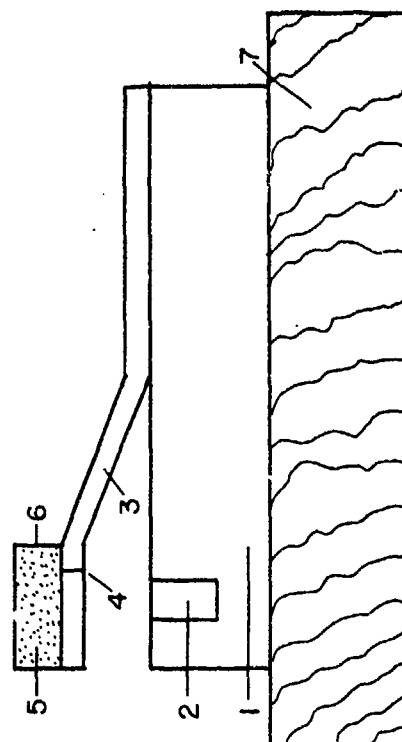
The experimental setup from Reference 18 is shown schematically in Figure 2a. Two plates, 1 and 3, of the same metal were prepared as follows. In the upper, usually thinner plate 3, they drilled a hole $0.3\text{-}0.5 \text{ mm}$ in diameter into which a wire 4 of the same material was tightly pressed. Into a rectangular slot extending across the entire

A



1. Metal plate
2. Plate inserted into rectangular slot
3. Metal plate
4. Wire inserted into cylindrical hole

B



5. Explosive charge
6. Detonator and detonation front
7. Wooden base

Figure 2. Diagram of the experimental setup (Reference 18).

width of plate 1, they inserted a plate 2 of exactly the same thickness as the slot. To improve the definition of the boundary and eliminate air gaps, steel specimens 1 and 2 were soldered with copper and copper specimens with silver solder in a vacuum. The space between aluminum specimens 1 and 2 was filled with epoxy resin. The thickness of the filler did not exceed 0.05 mm.

The plates 1 and 3, thus prepared, were mounted on a wooden base 7. Plate 3 was accelerated by the explosion products resulting from the detonation of the charge 5 (detonator 6) and driven against plate 1 (see Figure 2A). The impact (see Figure 2B, detonation front 6) usually resulted in the explosion welding of plates 1 and 3.

The monolithic specimens obtained after welding were cut in the direction of motion of the contact point velocity and thin sections were prepared. On macrophotographs of these sections, the horizontal displacement, z , of the boundary with respect to its original position, was measured as a function of the distance to the interface between the two welded plates, y ¹⁸.

The conservation of momentum for the collision of two plates, the experimental dependence of z versus y , and the steady-state, incompressible, viscous, Navier-Stokes equation enables one to estimate the metal viscosity coefficients¹⁸. These viscosity coefficients increase from aluminum through copper to steel. The maximum value of the viscosity coefficient for steel (steel 3) is

$$\mu = (3.9-4.8) \times 10^4 \text{ Pa-s},$$

for copper (M3) the viscosity is about one-half as large:

$$\mu = (2-2.7) \times 10^4 \text{ Pa-s},$$

whereas for aluminum (D16) the viscosity is an order-of-magnitude less than for steel:

$$\mu = (0.31-0.86) \times 10^4 \text{ Pa-s}.$$

These viscosity values for aluminum coincide with the results of References 21 and 23, and the viscosity values for steel agree with the results of References 2 and 3. The viscosity coefficients obtained disagree with the results of References 1 - 3 for aluminum, which predict a value of the order of 10^4 Pa-s, approximately the same as for steel, and there also exists a discrepancy with the data of References 21 and 23 for steel. In References 21 and 23 the viscosity of aluminum, copper, and steel are the same (10^3 Pa-s) but an order-of-magnitude less than the values given in References 1 - 3. According to Godunov¹⁸, the data of References 21 and 23, which found the viscosity values of very different materials to be nearly the same, are suspect. In the opinion of Reference 18, the constancy of the flow behind the front of the sinusoidal shock wave in Reference 23 was not always realized.

Next, Korsunskii²² used several theoretical methods to calculate the dynamic viscosity of liquids displaying metallic properties. This data, presenting both theoretical and experimental molten metal viscosity values, are given in Table IIIA. Table IIIB gives viscosity data for molten sodium as a function of temperature.

Mali¹⁹ quotes kinematic viscosity (ν/ρ) values taken from References 18 and 37. The kinematic viscosity was given as $2.5\text{m}^2/\text{s}$ for copper, $2.5\text{m}^2/\text{s}$ for duraluminum (D16), $1.0\text{m}^2/\text{s}$ for aluminum, $0.5\text{m}^2/\text{s}$ for lead, and $5.5\text{m}^2/\text{s}$ for steel. By assuming a constant density, the dynamic viscosities become 2.2×10^4 Pa-s for copper, 0.7×10^4 Pa-s for duraluminum, 0.3×10^4 Pa-s for aluminum, 0.6×10^4 Pa-s for lead, and 4.3×10^4 Pa-s for steel.

Table IV, taken from Godunov²⁴, lists values of ν , the kinematic viscosity, and $\dot{\epsilon}$ for aluminum and steel obtained by analyzing experimental data from the generation of planar flows formed by the oblique impact of explosively driven plates. The dynamic viscosity is also given in Table IV and was obtained by assuming incompressible flow. The viscosity coefficients were determined based on the assumption that decreases in the flow rate in comparison to the rate predicted by jet collapse theory (for small values of the collision angle and stagnation point velocity) occur because of the action of viscous forces. Godunov²⁴ also gives formulae for the variation of strain rate with temperature and for the Maxwellian viscosity as a function of temperature.

Godunov⁴ summarized the viscosity measurements discussed in the references cited above. From Godunov⁴, the deformation of a material depends essentially on the load acting on it as well as the rate of its application. At present, the range of low strain rates, achievable from existing tension test machines, have been investigated in detail where the strain rate can vary from 10^{-4} to 10^3 s⁻¹. Shock tests with explosives permit strain rates of 10^3 to 10^8 s⁻¹ to be obtained.

The viscoplastic solid model was used by References 1 and 3 in the analysis of experiments designed to determine the coefficient of viscosity of aluminum and steel for $\dot{\epsilon} = 10^3$ s⁻¹. The method of determining the viscosity of metals during explosive welding is described in Reference 18. The strain rates used in these tests were between 5×10^3 - 3×10^4 s⁻¹.

In Reference 5, a method was presented to determine the viscosity of metals during the symmetric oblique collision of plates in the mode where reverse jets exist. In this case, the jet velocities obtained experimentally were compared with the velocities computed by the viscous deceleration model. In this case, estimates of the coefficients of viscosity of diverse metals were carried out in the 10^5 - 10^7 s⁻¹ range of strain rates. The results obtained under the conditions of oblique collisions of metal plates are in good agreement with the results of References 21 and 23, where the development of small perturbations on

TABLE IIIA. CALCULATED AND EXPERIMENTAL VISCOSITIES
OF SEVERAL MOLTEN METALS NEAR THE MELTING POINT.
(Reference 22)

Metal	μ Theoretical $\times 10^3$ Pa-s	μ Experimental $\times 10^3$ Pa-s
Li	.28 - .44	.59
K	.83 - 3.6	.52
Mg	2.0	1.3
Zn	1.1 - 2.9	2.8
Cd	3.6	2.4
Hg	1.64	1.54
Al	1.8 - 2.5	1.2
Ga	1.9	1.9
In	4.3	1.65
Si	2.9	2.0
Sn	1.7	1.8
Pb	4.8 - 6.1	2.6
Sb	3.8	1.5
Bi	2.4	1.7

TABLE IIIB. VISCOSITY OF MOLTEN SODIUM AS A
FUNCTION OF TEMPERATURE. (Reference 22)

Temperature ($^{\circ}$ K)	μ Theoretical $\times 10^3$ Pa-s	μ Experimental $\times 10^3$ Pa-s
373	1.4 - 2.7	0.69
443	1.1 - 2.0	0.5
473	0.9 - 1.66	0.44
513	0.8 - 1.5	0.39

TABLE IV. VISCOSITY AS A FUNCTION OF STRAIN RATE,
GODUNOV (Reference 24)

<u>Steel 3</u>		
$\dot{\epsilon} \times 10^{-5} (\text{s}^{-1})$	$v (\text{m}^2/\text{s})$	$\mu (\text{Pa-s}) \times 10^{-3}$
3.3	4	31.4
7.2	3	23.5
7.5	2.5	19.6
15.2	1.8	14.1
27.5	1.3	10.2
58.5	1.3	10.2
137.0	1.2	9.4

<u>Aluminum</u>		
7	5	13.9
6.9	4.6	12.8
12	3.7	10.3
21.2	3.1	8.6
39	2.9	8.1
97	1.9	5.3

the shock front was studied for the same range of strain rates.

Figure 3, taken from Godunov⁴, shows the variation of experimental viscosity coefficients of steel and aluminum with strain rate. For strain rates greater than 10^4 s^{-1} , the viscosity coefficient of aluminum and steel depends weakly on strain rate, i.e., the viscosity decreases by about a factor of ten as the strain rate increases from 10^4 s^{-1} to 10^7 s^{-1} . Thus, the metals can be considered approximately as Newtonian fluids. The viscosity increases rapidly as the strain rate decreases below 10^4 s^{-1} . The viscosity data in Figure 3 was taken from References 1, 3, 21 and 23 at strain rates above 10^3 s^{-1} . The viscosity values at strain rates below 10^3 s^{-1} were taken from Reference 39 for tests involving rolling of the metal with preheating to 1273°K and stamping of the metal at 1273°K as reported in Reference 4.

Other USSR viscosity data was reported by Bakhsian¹⁷, who quoted a dynamic viscosity coefficient of armor steel as $3.9 \times 10^4 \text{ Pa-s}$. Also, Ivanov²⁵ studied the plastic deformation of soft steel tubes by detonating spherical charges of explosive placed in the central cross section of the tubes. The strain rates obtained in this test ranged from 10^3 to 10^5 s^{-1} . The viscosity values obtained by Ivanov²⁵ were claimed to be in agreement with the viscosity values obtained by other methods such as References 1, 2 and 37. The soft steel viscosity values were given as $2-5 \times 10^4 \text{ Pa-s}$ by Reference 25[†].

Shlykov³⁸ found that the kinematic viscosity of copper alloys varied strongly with temperature and composition. These copper alloys were investigated experimentally in the liquid stage. The alloys employed were Cu-Zn-Si, Cu-Zn, and Cu-Si with up to 50% Zn and up to 12% Si. The concentration dependence of Si (in Cu-Si alloys) on the kinematic viscosity is quite complex. Small concentrations of Si increase the kinematic viscosity. Larger amounts of Si cause the viscosity to decrease, and still larger amounts of Si cause the kinematic viscosity to increase again³⁸.

The US investigators: LASL, SANDIA Laboratory, and Lawrence Livermore Laboratory, have measured dynamic viscosities under explosive loading conditions to be of the order 10^2 Pa-s , typically lower than the measured USSR viscosity values. Swanson²⁹ studied the effects of strain-hardening and strain-rate treatments on one-dimensional calculations of aluminum response during plate impact experiments. For strain-rate effects on aluminum, a dynamic viscosity of 200 Pa-s was shown to best represent the free-surface velocity versus time behavior and the observed attenuation of thin pulses by rarefaction waves during the

[†]The units given by Ivanov²⁵ are kg f/m^2 , which are not dynamic viscosity units. The author has assumed that Ivanov means kg f-s/m^2 . Viscosities of order 10^4 Pa-s are then in agreement with the viscosities given by other USSR scientists as claimed by Ivanov²⁵.

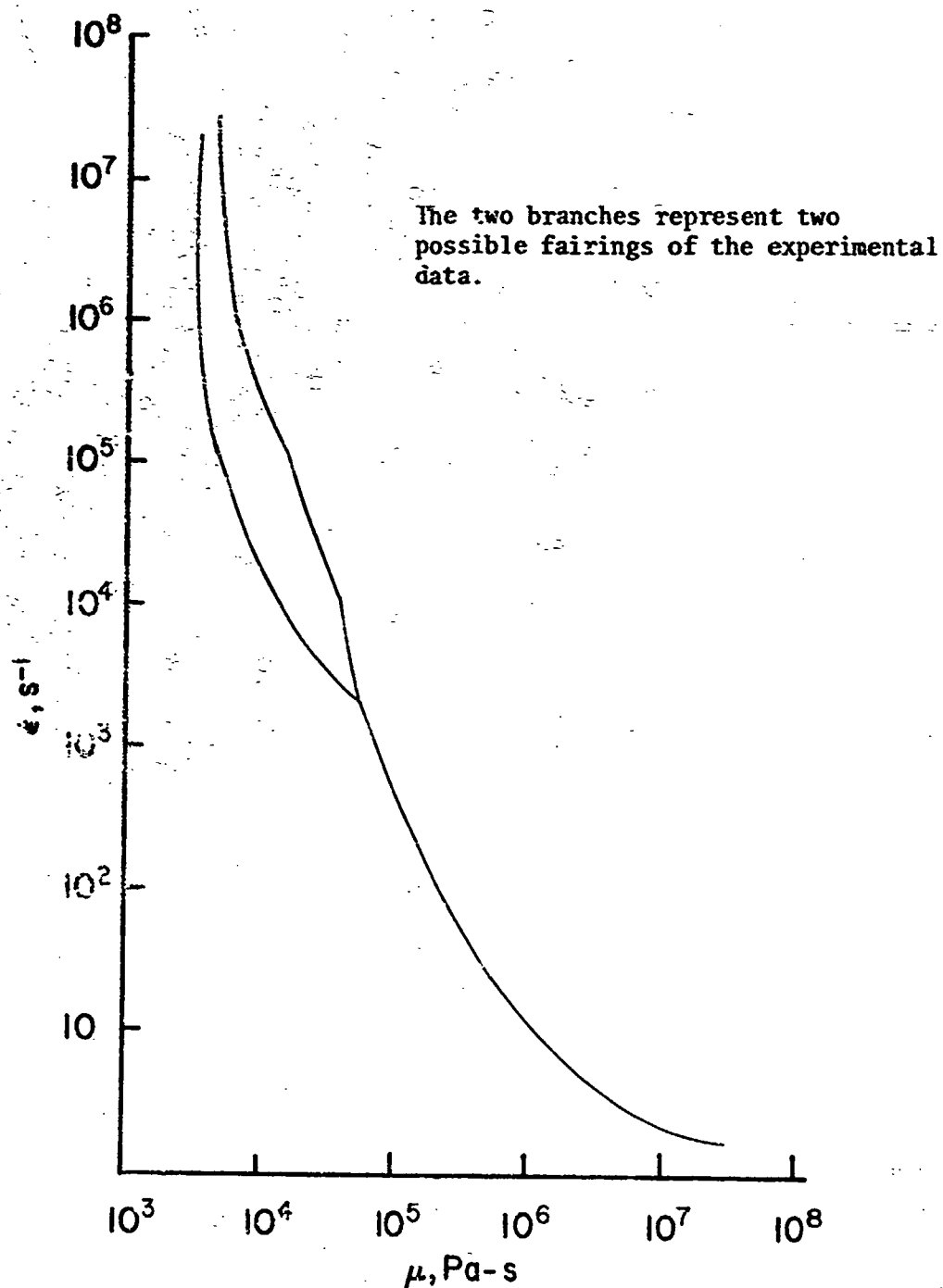


Figure 3. Measurements of the dynamic viscosity coefficient for different strain rates, Godunov (Reference 4).

plate impact experiments. Strain-hardening effects were shown to be secondary, but complementary, to the effects of viscosity. Pressure and temperature dependent relationships for the yield strength and shear modulus showed only minor effects and were concluded to be of secondary importance. Swanson²⁹ noted that the dynamic viscosity value is associated with the movement of dislocations that occur only after the yield stress has been reached. Dislocation dynamics, for shock impact experiments, have been studied by many USA researchers, notably, Asay^{40,41}, Taylor⁴², Gilman^{43,44}, Smith⁴⁵, and Lipkin⁴⁶. In the USSR crack propagation and dislocation theory was studied by Finkel^{47,48} and Golovin⁴⁹.

Gilman³⁰ theoretically calculated the approximate dynamic viscosity for strong shock waves in metals and concluded that the dynamic viscosity should be of the order of 0.1 Pa-s, whereas the viscosity of liquid metals is of the order of 5×10^{-3} Pa-s.

Finally, Barnes²⁸ in Figure 4, shows the variation of dynamic viscosity with pressure. Barnes comments that viscosity would appear to be important in mitigating shock perturbation growth, but the value of the viscosity coefficient is highly uncertain. In Figure 4, the viscosity data at high pressures is from the USSR experiments²¹, and the data at 200 Pa-s is from Swanson²⁹. The point below Swanson's results from fitting Barnes' experimental data on Taylor's growth in aluminum⁵⁰ with a viscous flow model. G. N. White actually used the viscous flow model to fit Barnes' data (see Reference 28). Also, recall that Gilman³⁰ calculated an upper limit of the viscosity in stressed metals to be 0.1 Pa-s.

Asay⁵¹ has deduced stressed metal dynamic viscosities by measuring shock rise times via velocity interferometry. The viscosity values given below represent an upper limit based on shock transition times. The time resolution is limited to 1 to 3 nanoseconds. The maximum stress is assumed proportional to the strain rate, $\sigma \sim \mu \dot{\epsilon}$, and the maximum stress is determined between the Rayleigh line and the shock Hugoniot pressure. The strain rate is calculated as the strain induced by the shock divided by the shock rise time, which is resolution limited. The calculated viscosity values are listed below.

Material	Pressure, Pa $\times 10^{-8}$	Dynamic Viscosity, Pa-s
Cu	~ 930	$\sim 3 \times 10^2$
Al	~ 450	$\sim 1 \times 10^2$
4340 Steel	~ 930	$\sim 6 \times 10^2$

Also, Harrison⁵² is currently computer modeling the USSR high-pressure experiments in order to resolve the strong variation in the quoted viscosity values especially regarding the value of 10^4 Pa-s quoted by the USSR versus the 10^2 Pa-s viscosity values quoted by the USA.

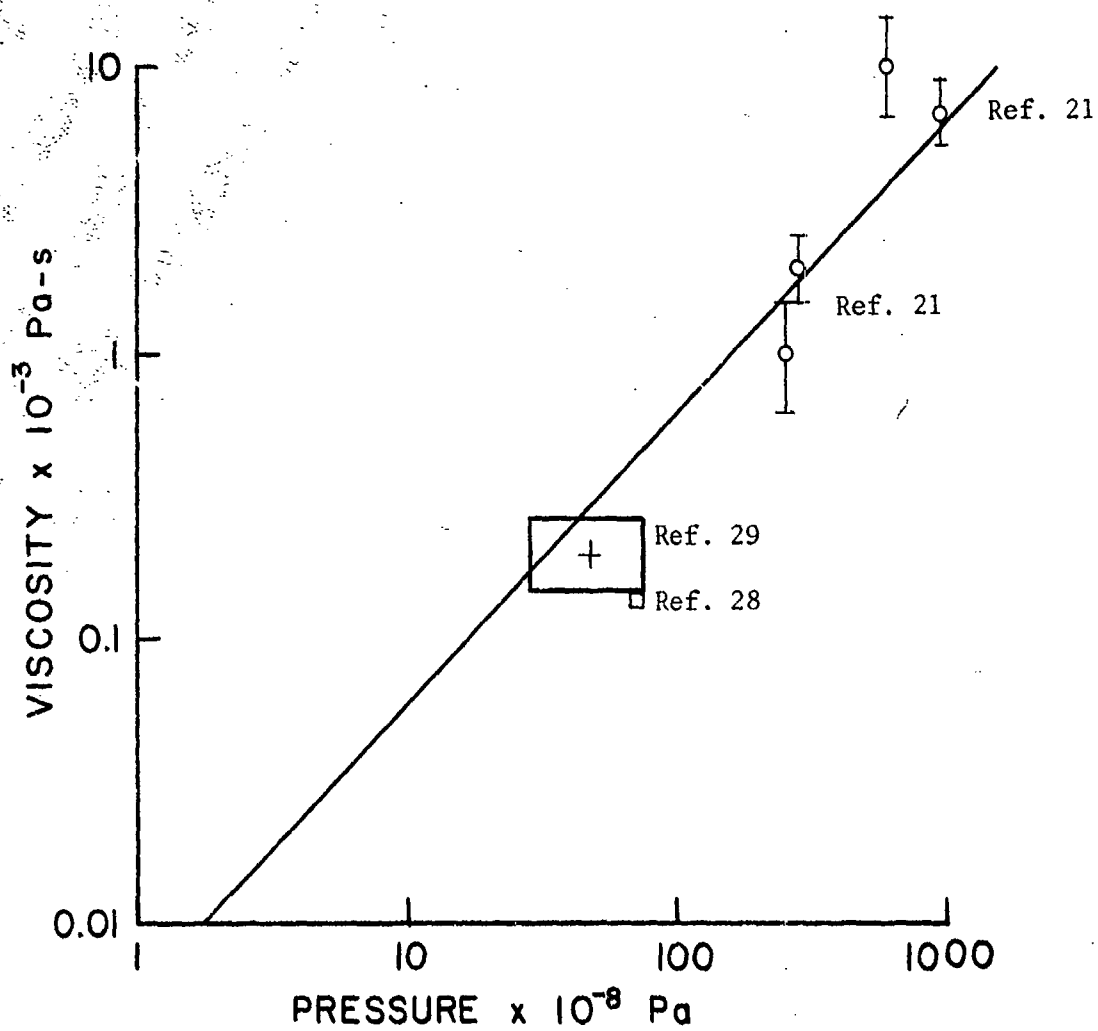


Figure 4. Dynamic viscosity versus pressure, Barnes (Reference 28).

Additional data in the open literature considers factors related to viscosity, although viscosity coefficients are not directly employed. These factors are thermal effects during impact from Belyakov^{53,54}, the effect of temperature on the mechanical properties of metals from Sazonov⁵⁵ and Sklyuev⁵⁶, explosive effects on plate acceleration from Godunov⁵⁷ and Trofimov⁵⁸, and the mechanical properties of metals under dynamic conditions from Yakhnin⁵⁹, Tass⁶⁰, Men'shikov⁶¹, and Wilkins⁶². References 61 and 62 treated elastic-plastic, stress-strain models with strain hardening considerations in order to determine the dynamic yield strength of rods of various materials impacting rigid targets. Wilkins lists the calculated dynamic yield strength of several materials including aluminum, steel, copper, uranium, tantalum, magnesium alloys, and beryllium alloys.

It is interesting to note that Moss⁶³ of BRL/ARRADCOM experimentally obtained viscosity data from void growth measurements. Dr. Moss obtained dynamic viscosity values of 357 Pa-s for 1/2-inch thick (12.7 mm) RHA plate and 20 Pa-s for copper. The viscosity value for the RHA plate includes some effects of void coalescence but is in general agreement with the value given by Asay⁵¹. The viscosity value for copper is lower by about an order-of-magnitude over Asay's value. However, the exact test conditions (thermodynamic properties) of the test specimens are not known.

IV. SUMMARY AND CONCLUSIONS

The USA, for the most part, assumes elastic-perfectly plastic or strain hardening models for the constitutive relationships used in the hydrocode calculations. The USSR, on the other hand, contends that viscous effects are at least as important as compressibility effects in the jet collapse process. Thus, the USSR constitutive relationships utilize a visco-plastic, stress-strain rate model where the stress is assumed proportional to the strain rate and with the factor of proportionality being the dynamic viscosity coefficient. The viscosity coefficient is assumed to be constant, but this is true only for a given pressure, temperature, and strain rate.

The USSR measured the viscosity coefficients for the propagation of shock waves through several materials. The viscosity of all shock loaded materials is of the same order-of-magnitude. For metals, the dynamic viscosity coefficient was in the range of 10^3 to 10^5 Pa-s. The US investigators typically measure dynamic viscosities of the order of 10^2 Pa-s. The estimate of the viscosity coefficient from measured values undoubtedly depends on the experimental procedure employed as well as the experimental accuracy. Theoretical viscosity coefficients are about 0.1 Pa-s, and liquid metal viscosity coefficients are of the order 10^{-3} Pa-s. The differences in the viscosity values between the USSR and USA might be attributed to pressure differences, Barnes²⁸ (see Figure 4). Strain rate also influences the

viscosity as shown by Godunov⁴ (see Figure 3). Temperature also influences the viscosity strongly, especially near the melt point.

In short, as stated by Barnes²⁸, "Viscosity would appear to be a very important factor in mitigating perturbation growth, but the value of viscosity coefficient is highly uncertain."

It seems to this author that further research in this area is required to determine the dependence of the viscosity coefficient on pressure, temperature, and strain rate as well as to increase the accuracy of the viscosity measurement. Viscous effects should definitely be an important mechanism in dissipating shock-wave fronts during the shaped-charge jet formation and the jet penetration process.

Viscous effects can be incorporated into the jet calculations (for example, Walters⁶⁴), but the coefficient of dynamic viscosity must be known. The problem is further complicated by the dependence of the viscosity on both the pressure and temperature, since good equation-of-state data and accurate temperature calculations are currently not available for problems involving the explosive loading of metals.

V. RECOMMENDATIONS

Visco-plastic or rate-dependent models should be investigated in regard to the possibility of improving shaped-charge jet collapse, formation, and penetration calculations.

The one-dimensional, incompressible, steady-state model for the jet velocity given by Godunov⁴, which is analogous to the Pugh-Eichelberger-Rostoker model except that viscous effects have been included, should be analyzed. In particular, the jet-no-jet criterion proposed by Godunov, which is based on a critical Reynolds number, should be checked against the USA data. A critical Reynolds number criterion on the jet-no-jet conditions is more meaningful than a critical Mach number criterion for incompressible flow models. The necessary equations are given in this report.

ACKNOWLEDGMENT

The author is grateful to Mr. James Byrnes of the BRL Foreign Intelligence Office for his patient and methodical search of the Russian literature and the acquisition of most of the Russian documents referenced in this report.

The author is grateful to T. Neal, J. Barnes, and K. Harrison of LASL, J. Asay of Sandia Laboratory, and J. Shaner of Lawrence Livermore Laboratory for many interesting discussions and the release of unpublished data.

REFERENCES

1. A. A. Il'yushin, Uch. Zap. MGU, Mekhan., 39, NO. 11 (1940).
2. A. A. Il'yushin, "Metal Testing at High Velocities," Inzh. Sb., 1, No. 1, (1941).
3. S. M. Popov, Inzh. Sb., 1, No. 1, 1941.
4. S. K. Godunov, A. A. Deribas and V. I. Mali, "Influence of Material Viscosity on the Jet Formation Process During Collisions of Metal Plates," Fizika Goreniya i Vzryva, Vol. 11, No. 1, Jan-Feb., 1975.
5. S. K. Godunov and A. A. Deribas, "Jet Formation Upon Collision of Metals," Doklady Akademii Nauk SSSR, Vol. 202, No. 5, Feb 1972.
6. A. A. Deribas, V. M. Kudinov, F. I. Matveenkoy and V. A. Simonov, "Determination of the Impact Parameters of Flat Plates in Explosive Welding," Fizika Goreniya i Vzryva, Vol. 3, No. 2, 1967.
7. N. P. Novikov, "Certain Properties of High-Speed Cumulative Jets," Zh. Prikladnoy Mekhaniki i Tekhnicheskoy Fiziki, No. 1, 1963.
8. V. A. Simonov, "Flows Due to an Incident Impact Wave on a Wedge-Shaped Cavity," Fizika Goreniya i Vzryva, Vol 7, No. 2, April-June, 1971.
9. S. K. Godunov, A. A. Deribas, A. V. Zabrodin and N. S. Kozin, "Hydrodynamic Effects in Colliding Solids," J. of Computational Physics, V. 5, 1970.
10. G. Birkhoff, D. P. Mac Dougall, E. M. Pugh and G. Taylor, "Explosives with Lined Cavities," J. Appl. Physics, Vol. 19, No. 6, June 1948.
11. E. M. Pugh, R. J. Eichelberger and N. Rostoker, "Theory of Jet Formation by Charges with Lined Conical Cavities," J. Appl. Physics, Vol. 23, No. 5, May 1952.
12. M. Defourneaux, "Hydrodynamic Theory of Shaped Charges and of Jet Penetration, Memorial De L'artillerie Francasise-T, 44, 1970. (Translation by M. Lampson, BRL).
13. P. C. Chou, J. Carleone and R. R. Karpp, "Criteria for Jet Formation from Impinging Shells and Plates," J. Appl. Physics, Vol. 47, No. 7, July 1976.
14. J. Harrison, R. DiPersio, R. Karpp and R. Jameson, "A Simplified Shaped Charge Computer Code: BASC," DEA-AF-F/G-7304 Technical Meeting: Physics of Explosives, Vol. II, April-May 1974, Paper 13 presented at the Naval Ordnance Laboratory, Silver Spring, MD.

REFERENCES

15. N. Cristescu, Dynamic Plasticity, Chapter X, John Wiley & Sons, Inc., New York, 1967.
16. G. I. Barenblatt and A. Iu. Ishlinskii, "On the Impact of a Visco-Plastic Bar on a Rigid Obstacle," PMM, Vol. 26, No. 3, 1962.
17. F. A. Bakhsiiyan, "Visco-Plastic Flow in a Plate Produced by a Shock with a Cylinder, Prikl. Mat. Makh., 12, No. 1, 1948.
18. S. K. Godunov, A. A. Deribas, I. D. Zakharenko and V. I. Mali, "Investigation of the Viscosity of Metals in High-Velocity Collisions," Fizika Goreniya i Vzryva, No. 1, pp. 135-141, Jan-March, 1971.
19. V. I. Mali, V. V. Pai and A. I. Skovpin, "Investigation of the Breakdown of Flat Jets," Fizika Goreniya i Vzryva, Vol. 10, No. 5, Sept-Oct, 1974.
20. V. N. Mineev and R. M. Zaidel, "The Viscosity of Water and Mercury Under Shock Loading," Soviet Physics JETP, Vol. 27, No. 6, December, 1968.
21. V. N. Mineev and F. V. Savinov, "Viscosity and Melting Point of Aluminum, Lead and Sodium Chloride Subjected to Shock Compression," Soviet Physics JETP, Vol. 25, No. 3, Sept. 1967.
22. A. M. Korsunskii, V. E. Sivolap and A. G. Bondareva, "Hard-Sphere Model and Viscosity of Liquid Metals," Izvestiya Vysshikh Uchebnykh Zavedenii, Fizika, No. 3, March, 1975.
23. A. D. Sakharov, R. M. Zaidel, V. N. Mineev and A. G. Oleinik, "Experimental Investigation of the Stability of Shock Waves and the Mechanical Properties of Substances at High Pressures and Temperatures," Soviet Physics - Doklady, Vol. 9, No. 12, June, 1965.
24. S. K. Godunov, A. F. Demchuk, N. S. Kozin and V. I. Mali, "Interpolation Formulas for Maxwell Viscosity of Certain Metals as a Function of Shear-Strain Intensity and Temperature," Zhurnal Prikladnoi Mekhaniki i Tekhnicheskoi Fiziki, No. 4, July-August, 1974.
25. A. G. Ivanov, "Explosive Deformation and Destruction of Tubes," Problemy Prochnosti, No. 11, Nov. 1976.
26. Arthur Burkhardt, Erhard Hornbogen and Karl Keller, "Übergang zu Turbulentem Fließen in Kristallen," Z. Metallkunde, Vol. 58, No. 6, 1967.

REFERENCES

27. F. H. Harlow and W. E. Pracht, "Formation and Penetration of High-Speed Collapse Jets," *Physics of Fluids*, Vol. 9, No. 10, Oct 1966.
28. John F. Barnes, "Surface Instabilities Under Shock-Wave Loading," LA-UR-78-188, Los Alamos Scientific Laboratory, Synopsis of a paper presented at the San Francisco American Physical Society Meeting, 23-26 January 1978.
29. R. E. Swanson and C. L. Mader, "One-Dimensional Elastic-Plastic Calculations Involving Strain-Hardening and Strain-Rate Effects for Aluminum," Los Alamos Scientific Laboratory, UC-32, May 1975.
30. J. J. Gilman, "Resistance to Shock Front Propagation in Solids," review copy of article to be published.
31. J. Walsh, R. Shreffler and F. Willig, "Limiting Conditions for Jet Formation in High Velocity Collisions," *J. Appl. Physics*, 24, No. 3, 1953.
32. L. M. Milne-Thomson, *Theoretical Hydrodynamics*, Fourth Edition, The Mac Millan Company, N.Y., 1960, Chapter 11.
33. L. A. Al'tshuler, S. B. Kormer, et al., *Zh. ETF*, 38, No. 4, 1061 (1960) [*Soviet Physics - JETP*, Vol 11, p. 766].
34. S. B. Kormer, A. I. Funtikov, V. D. Urlin and A. N. Kolesnikova, *JETP* 42, 686 (1962), *Soviet Physics, JETP* 15, 477, 1962.
35. L. V. Al'tshule: . A. Bakanova and R. F. Trunin, *JETP* 42, 91 (1962) *Soviet Physics JETP* 15, 65 (1962).
36. S. B. Kormer, M. V. Sinitsyn, G. A. Kirillov and V. D. Urlin, *JETP* 48, 1033 (1965), *Soviet Physics JETP* 21, 689 (1965).
37. I. D. Zakharenko and V. I. Mali, *Combustion and Explosion* (in Russian), Izd. Nauka, Moscow, 1972.
38. A. V. Shlykov, V. M. Chursin, "Investigation of the Kinematic Viscosity of Alloys of the Cu-Si-Zn System," *Izv. Vys. Ucheb. Zaved., Tsvetnaya Metallurgiya*, No. 6, 1976.
39. W. Klein, in *Third International Conference of the Center for High-Energy Forming*, July 12-16, 1971, Vail, Colorado.
40. J. R. Asay, G. R. Fowles, G. E. Durall, M. H. Miles and R. F. Tinder, "Effects of Point Defects on Elastic Precursor Decay in LiF," *J. of Applied Physics*, Vol. 43, No. 5, May 1972.

REFERENCES

41. J. R. Asay, D. L. Hicks and D. B. Holdridge, "Comparison of Experimental and Calculated Elastic-Plastic Wave Profiles in LiF," J. of Applied Physics, Vol. 46, No. 10, Oct. 1975.
42. John W. Taylor, "Dislocation Dynamics and Dynamic Yielding," J. of Applied Physics, Vol 36, No. 10, Oct. 1965.
43. J. J. Gilman, "Dislocation Motion in a Viscous Medium," Physical Review Letters, Vol. 20, No. 4, 22 Jan 1968.
44. J. J. Gilman, "Dislocation Dynamics and the Response of Materials to Impact," Applied Mechanics Reviews, Vol. 21, No. 8, August 1968.
45. Cyril Stanley Smith, "Metallographic Studies of Metals after Explosive Shock," Transactions of the Metallurgical Society of AIME, Oct, 1958.
46. J. Lipkin and J. R. Asay, "Shock and Release of Shock-Compressed 6061-T6 Aluminum," J. Appl. Physics, Vol. 48, No. 1, Jan 1977.
47. V. M. Finkel, G. B. Muravin, L. S. Rozinskiy, A. M. Savel'yev and L. M. Lezvinskaya, "On the Slowing Down of Fast Cracks in Silicon Iron," Fizika Metallov I Metal-lovedenie, Vol. 40, No. 5, 1975.
48. V. M. Finkel, L. N. Muratova, Yu. I. Tyalin, G. A. Baryshev and M. N. Golzman, "Fault Band as a Barrier to Cracks," Fizika Metallov I Metallovedenie, Vol. 41, No. 1, 1976.
49. Yu. I. Golovin, V. M. Finkel and A. A. Sletkov, "Effects of Current Pulses on Crack Propagation Kinetics in Silicon Iron," Problemy Prochnosti, No. 2, Feb. 1977.
50. John F. Barnes, P. J. Blewett, R. G. McQueen, K. A. Meyer and D. Venable, "Taylor Instability in Solids," J. of Applied Physics, Vol. 45, No. 2, Feb 1974.
51. J. R. Asay, Sandia Laboratories, Private communication.
52. Katy Harrison, LASL, Private communication.
53. L. V. Belyakov, V. P. Valitskii and N. A. Zlatin, "Thermal Phenomena Arising in Impact of a Projectile on a Metal Surface," Zhurnal Tekhnicheskoi Fiziki, Vol. 36, No. 10, Oct. 1966.
54. L. V. Belyakov, V.P. Valitskii and N. A. Zlatin, "The Role of Thermal Phenomena in Collisions of Metallic Bodies," Soviet Physics-Doklady, Vol. 10, No. 1, July 1965.

REFERENCES

55. B. G. Sazonov and I. A. Drozdova, "Effects of Heating on the Mechanical Properties of Previously Quenched Steels," *Metallovedenie i Termicheskaya Obrabotka Metallov*, No. 7, July, 1976.
56. P. V. Skyuev, "Effect of Cooling Rate and Supercooling Temperature on the Fracture Toughness and Transition Temperature of Steels 35 KhNM and 34 Khn3M," *Metallovedenie i Termicheskaya Obrabotka Metallov*, No. 8, August, 1977.
57. S. K. Godunov, Ya. M. Kazhdan and V. A. Simonov, "Shock Wave Incidence on a V-Shaped Cavity," *Zhurnal Prikladnoi Mekhaniki i Tekhnicheskoi Fiziki*, Vol. 10, No. 6, Nov-Dec., 1969.
58. V. S. Trofimov, "Elementary Technique for Estimating the Parameters of a High-Explosive Charge for the Plane Acceleration of a Metal Plate," *Fizika Goreniya i Vzryva*, Vol. 12, No. 1, Jan-Feb., 1976.
59. A. S. Yakhnin, "Relationship Between Impact Strength and Form of Fracture of Constructional Steels in the Zone of Brittle-Ductile Transition," *Zavodskaya Laboratoriya*, Vol. 43, No. 6, June, 1977.
60. TASS, "Improvement of the Properties of Metals," *Nauka i tekhnika*, No. 37, Sept. 17, 1977, p. 3.
61. G. P. Men'shikov, V. A. Odintsov and L. A. Chudov, "Cylindrical Striker Penetration Into Finite Plate," *I zu. AN SSSR. Mekhanika Tverdogo Tela*, Vol. 11, No. 1, 1976.
62. M. L. Wilkins and Micahel W. Guinan, "Impact of Cylinders on a Rigid Boundary," *J. of Applied Physics*, Vol. 44, No. 3, March 1973.
63. Gerald Moss, Ballistics Research Laboratories, Private communication, March, 1979.
64. Walters, W. P., "Axially Symmetric Incompressible Shaped-Charge Jets," Technical Report ARBRL-TK-02045, Feb. 1978. (AD #A051053)

DISTRIBUTION LIST

<u>No. of</u> <u>Copies</u>	<u>Organization</u>	<u>No. of</u> <u>Copies</u>	<u>Organization</u>
2	Commander Defense Documentation Center ATTN: DDC-DDA Cameron Station Alexandria, VA 22314	1	Commander US Army Tank Automotive Research & Development Cmd ATTN: DRDTA-UL Warren, MI 48090
1	Commander US Army Materiel Development and Readiness Command ATTN: DRCDMD-ST 5001 Eisenhower Avenue Alexandria, VA 22333	8	Commander US Army Armament Research and Development Command ATTN: DRDAR-TSS (2 cys) Mr. T. Stevens Mr. G. Randers-Pehrson Dr. N. Clark Mr. J. Hershkowitz Mr. J. Pearson LCU-CT, Mr. E. Yuhas Dover, N.J. 07801
1	Commander US Army Aviation Research and Development Command ATTN: DRSAB-E P.O. Box 209 St. Louis, MO 63166	1	Commander US Army Armament Materiel Readiness Command ATTN: DRSAR-LEP-L, Tech Lib Rock Island, IL 61299
1	Director US Army Air Mobility Research and Development Laboratory Ames Research Center Moffett Field, CA 94035	2	Commander US Army Materials and Mechanics Research Center ATTN: DRXMR-RF, J. Mescall Tech Lib Watertown, MA 02172
1	Commander US Army Electronics Research and Development Command Technical Support Activity ATTN: DELSD-L Fort Monmouth, NJ 07703	1	Director US Army TRADOC Systems Analysis Activity ATTN: ATAA-SL, Tech Lib White Sands Missile Range NM 88002
1	Commander US Army Communications Rsch and Development Command ATTN: DRDCO-PPA-SA Fort Monmouth, NJ 07703	1	Assistant Secretary of the Army (R&D) ATTN: Asst for Research Washington, DC 20310
2	Commander US Army Missile Research and Development Command ATTN: DRDMI-R DRDMI-YDL Redstone Arsenal, AL 35809		

DISTRIBUTION LIST

<u>No. of Copies</u>	<u>Organization</u>	<u>No. of Copies</u>	<u>Organization</u>
2	HQDA (DAMA-ZA; DAMA-AR) Washington, DC 20310	1	Commander Naval Research Laboratory Washington, DC 20375
1	Commander US Army Research Office P. O. Box 12211 Research Triangle Park NC 27709	1	USAF/AFRDDA Washington, DC 20311
2	Commander Naval Air Systems Command ATTN: Code AIR-310 Code AIR-350 Washington, DC 20360	1	AFSC/SDW Andrews AFB Washington, DC 20311
1	Commander Naval Ordnance Systems Command ATTN: Code ORD-0332 Washington, DC 20360	1	US Air Force Academy ATTN: Code FJS-41 (NC) Tech Lib Colorado Springs, CO 80840
2	Chief of Naval Research Department of the Navy ATTN: Code 427 Code 470 Washington, DC 20325	1	AFATL/DLJW (J. Foster) Eglin AFB, FL 32542
1	Commander Naval Surface Weapons Center ATTN: Code 730, Lib Silver Spring, MD 20910	1	AFWL (SUL, LT Tennant Kirtland AFB, NM 87116
2	Commander Naval Surface Weapons Center ATTN: Code DG-50 DX-21, Lib Br Dahlgren, VA 22448	1	AFLC/MMWMC Wright-Patterson AFB, OH 45433
2	Commander Naval Weapons Center ATTN: Code 4057 Code 45, Tech Lib China Lake, CA 93555	1	AFAL/WR Wright-Patterson AFB, OH 45433
		8	Director Lawrence Livermore Laboratory ATTN: Dr. J. Kury Dr. M. Wilkins Dr. E. Lee Dr. H. Horning Dr. J. Knowles Dr. M. Van Thiel Dr. C. Godfrey Tech Lib P.O. Box 808 Livermore, CA 94550
		1	Battelle-Columbus Laboratories ATTN: Mr. Joseph E. Backofen 505 King Avenue Columbus, OH 43201

DISTRIBUTION LIST

<u>No. of Copies</u>	<u>Organization</u>	<u>No. of Copies</u>	<u>Organization</u>
2	Dyna East Corporation ATTN: P. C. Chou J. Carleone 227 Hemlock Road Wynnewood, PA 19096	1	University of Dayton Research Institute ATTN: Dr. S. Bless Dayton, OH 45469
1	Firestone Defense Research and Products Division of the Firestone Tire and Rubber Co. ATTN: R. Berus 1200 Firestone Parkway Akron, OH 44317	1	University of Denver Denver Research Institute ATTN: Mr. R.F. Recht 2390 S. University Boulevard Denver, CO 80210
2	Honeywell, Inc. Government and Aeronautical Products Division ATTN: C. R. Hargreaves R. S. Kensinger 600 Second Street Hopkins, MN 55343	2	University of Illinois Dept. of Aeronautical and Astronautical Engineering ATTN: Prof. A. K. Zak Prof. S. M. Yen Urbana, IL 61801
2	Sandia Laboratories ATTN: Dr. W. Herrmann Dr. J. Asay Albuquerque, NM 87115	<u>Aberdeen Proving Ground</u>	
1	Shock Hydrodynamics ATTN: Dr. L. Zernow 4710-4716 Vineland Avenue North Hollywood, CA 91602	Dir, USAMSAA ATTN: Dr. J. Sperrazza B. Oeheli G. Johnson DRXSY-MP, H. Cohen	
1	Systems, Science & Software ATTN: Dr. R. Sedgwick P.O. Box 1620 La Jolla, CA 92037	Cdr, USATECOM ATTN: DRSTE-TO-F Dir, Wpns Sys Concepts Team, Bldg. E3516, EA ATTN: DRDAR-ACW	
6	University of California Los Alamos Scientific Lab ATTN: Dr. J. Walsh Dr. R. Karpp Ms. K. Harrison Dr. J. Barnes Dr. J. Sedan Tech Lib P.O. Box 1663 Los Alamos, NM 87544		

USER EVALUATION OF REPORT

Please take a few minutes to answer the questions below; tear out this sheet and return it to Director, US Army Ballistic Research Laboratory, ARRADCOM, ATTN: DRDAR-TSB, Aberdeen Proving Ground, Maryland 21005. Your comments will provide us with information for improving future reports.

1. BRL Report Number _____

2. Does this report satisfy a need? (Comment on purpose, related project, or other area of interest for which report will be used.)

3. How, specifically, is the report being used? (Information source, design data or procedure, management procedure, source of ideas, etc.) _____

4. Has the information in this report led to any quantitative savings as far as man-hours/contract dollars saved, operating costs avoided, efficiencies achieved, etc.? If so, please elaborate.

5. General Comments (Indicate what you think should be changed to make this report and future reports of this type more responsive to your needs, more usable, improve readability, etc.) _____

6. If you would like to be contacted by the personnel who prepared this report to raise specific questions or discuss the topic, please fill in the following information.

Name: _____

Telephone Number: _____

Organization Address: _____

